



Research paper

Systemic enzyme delivery by blood-brain barrier-penetrating SapC-DOPS nanovesicles for treatment of neuronopathic Gaucher disease



Ying Sun^{a,b,*}, Benjamin Liou^a, Zhengtao Chu^c, Venette Fannin^a, Rachel Blackwood^a, Yanyan Peng^a, Gregory A. Grabowski^a, Harold W. Davis^c, Xiaoyang Qi^{a,b,c,*}

^a Division of Human Genetics, Cincinnati Children's Hospital Medical Center, Cincinnati, OH, USA

^b Department of Pediatrics, University of Cincinnati College of Medicine, Cincinnati, OH, USA

^c Division of Hematology/Oncology, Department of Internal Medicine, University of Cincinnati, College of Medicine, Cincinnati, OH, USA

ARTICLE INFO

Article History:

Received 6 November 2019

Revised 6 March 2020

Accepted 10 March 2020

Available online 10 April 2020

Keywords:

Neurodegenerative disease

Central nervous system

SapC-DOPS nanovesicles

Enzyme replacement therapy

Neuronopathic Gaucher disease

Acid- β -glucosidase

ABSTRACT

Background: Enzyme replacement therapy (ERT) can positively affect the visceral manifestations of lysosomal storage diseases (LSDs). However, the exclusion of the intravenous ERT agents from the central nervous system (CNS) prevents direct therapeutic effects.

Methods: Using a neuronopathic Gaucher disease (nGD) mouse model, CNS-ERT was created using a systemic, non-invasive, and CNS-selective delivery system based on nanovesicles of saposin C (SapC) and dioleoylphosphatidylserine (DOPS) to deliver to CNS cells and tissues the corrective, functional acid β -glucosidase (GCase).

Findings: Compared to free GCase, human GCase formulated with SapC-DOPS nanovesicles (SapC-DOPS-GCase) was more stable in serum, taken up into cells, mostly by a mannose receptor-independent pathway, and resulted in higher activity in GCase-deficient cells. In contrast to free GCase, SapC-DOPS-GCase nanovesicles penetrated through the blood-brain barrier into the CNS. The CNS targeting was mediated by surface phosphatidylserine (PS) of blood vessel and brain cells. Increased GCase activity and reduced GCase substrate levels were found in the CNS of SapC-DOPS-GCase-treated nGD mice, which showed profound improvement in brain inflammation and neurological phenotypes.

Interpretation: This first-in-class CNS-ERT approach provides considerable promise of therapeutic benefits for neurodegenerative diseases.

Funding: This study was supported by the National Institutes of Health grants R21NS 095047 to XQ and YS, R01NS 086134 and UH2NS092981 in part to YS; Cincinnati Children's Hospital Medical Center Research Innovation/Pilot award to YS and XQ; Gardner Neuroscience Institute/Neurobiology Research Center Pilot award to XQ and YS, Hematology-Oncology Programmatic Support from University of Cincinnati and New Drug State Key Project grant 009ZX09102-205 to XQ.

© 2020 The Authors. Published by Elsevier B.V. This is an open access article under the CC BY-NC-ND license. (<http://creativecommons.org/licenses/by-nc-nd/4.0/>)

1. Introduction

Gaucher disease (GD) is a lysosomal storage disease with a frequency of 1/50,000 to 100,000 in general population [1, 2]. In GD, *GBA1* mutations lead to defective acid β -glucosidase (GCase) function and the accumulation of its substrates, glucosylceramide (GluCer) and glucosylsphingosine (GluSph), resulting in multi-organ dysfunction [1, 3]. Typical manifestations of GD type 1 include visceral, hematologic and bone disease reflected by hepatosplenomegaly,

anemia, thrombocytopenia and osteopenia/osteoporosis. In comparison, types 2 and 3 exhibit these visceral signs and also early onset progressive neuronopathic disease, i.e., nGD, with primary brain pathology characterized by neuronal necroptosis and inflammation [1, 4, 5]. Life expectancy is about 1–2 years for GD type 2 patients, and up to 30–40 years for those with GD type 3. *GBA1* mutations have also been identified as the most common genetic risk factor for Parkinson and Lewy body diseases [6–8].

Approved therapies for GD include enzyme replacement therapy (ERT; e.g., Imiglucerase, Velaglucerase alfa and Taliglucerase alfa) [9] and substrate reduction therapies (SRT; Miglustat and Eliglustat) [10]. These therapies have positive effects on the visceral manifestations of the GD variants [11, 12], but none have direct effects on the central nervous system (CNS) signs and symptoms [12–14]. A new

Work was conducted in Cincinnati, OH, USA.

* Corresponding author at: Division of Hematology/Oncology, Department of Internal Medicine, University of Cincinnati College of Medicine, and Division of Human Genetics, Cincinnati Children's Hospital Medical Center, Cincinnati, Ohio, USA.

E-mail addresses: ying.sun@cchmc.org (Y. Sun), Xiaoyang.qi@uc.edu (X. Qi).

<https://doi.org/10.1016/j.ebiom.2020.102735>

2352-3964/© 2020 The Authors. Published by Elsevier B.V. This is an open access article under the CC BY-NC-ND license. (<http://creativecommons.org/licenses/by-nc-nd/4.0/>)

Research in the context

Evidence before this study

Gaucher disease is a rare genetic disease caused by the mutations of *GBA1* gene encoding lysosomal enzyme, acid β -glucosidase (GCCase), and is classified as visceral (Type 1) or neuronopathic (Types 2 and 3). A major limitation of FDA approved enzyme replacement therapy (ERT) is failure to cross the blood-brain barrier (BBB). Therefore, the currently available treatments are only effective on the visceral manifestations of Gaucher disease and are completely ineffective for Types 2 and 3 neuronopathic central nervous system (CNS) variants that present often early in life with high mortality. A novel complex, saposin C (SapC) and dioleoyl-phosphatidylserine (DOPS) nanovesicles, has the ability to cross the BBB and selectively target neuronal tissue, providing a biological vehicle for delivering GCCase into the CNS.

Added value of this study

We demonstrate that a systemic CNS-selective delivery system using SapC-DOPS nanovesicles supplies functional GCCase to a variety of tissues, especially the brain. SapC-DOPS-GCCase, as a novel therapeutic approach, corrects GCCase deficiency in CNS cells and tissues and shows efficacy in reducing CNS inflammation and neurological phenotypes in a mouse model of neuronopathic Gaucher disease. Our study establishes a new mechanism of CNS targeting of SapC-DOPS through a specific phosphatidylserine receptor and the lymphatic circulation. This CNS-selective delivery system using SapC-DOPS nanovesicles provides a new strategy for treating neuronopathic Gaucher disease.

Implications of all the available evidence

This therapeutic approach utilizing SapC-DOPS nanovesicles to deliver the enzyme into the brain will advance CNS disease treatment in neuronopathic Gaucher disease. Although this study was focused on a rare disease, there may be ramifications for similar but vastly more common conditions such as Parkinson disease in which decreased GCCase activity has been documented in the patients' brains. As without improvements in treatment neuronopathic Gaucher disease will remain lethal, SapC-DOPS-GCCase has the potential to translate rapidly to improved patient care.

delivers SapC to extra-cranial inflammatory sites [29] and, by crossing the blood-brain barrier (BBB), to primary brain tumors and brain metastases of breast and lung cancers [30, 31]. Thus, SapC-DOPS nanovesicles are capable of enhancing mutant GCCase function, and also provide a biological vehicle for delivering GCCase into the CNS.

Here, a non-invasive delivery system for GCCase, i.e., SapC-DOPS nanovesicles, is shown to enhance GCCase function, supply functional GCCase to a variety of tissues, especially the brain, and demonstrates in vivo efficacy in improving CNS signs in a mouse model of nGD. This therapeutic approach to deliver the enzyme into the brain will advance CNS disease treatment in nGD.

2. Materials and methods

2.1. Materials

The following reagents were from commercial sources: condurit-B-epoxide (CBE), neurobasal, FJC staining kit (Fluoro-Jade® C), mouse anti-NeuN monoclonal antibody (MAB377), rat anti- β actin, -Lamp1 and -Lamp2a antibodies (EMD Millipore, Bedford, MA); mammalian protein extraction reagent (M-PER; Invitrogen), DMEM, RPMI medium and Pierce BCA protein assay kit (ThermoFisher Sci., Waltham, MA); rat anti-mouse LYVE1 monoclonal antibody (ALY7; eBioscience, Waltham, MA); mouse anti-GFAP monoclonal antibody (Clone2E1.E9) and mouse anti-Tuj1 monoclonal antibody (StemCell, Cambridge, MA); mouse anti-CD68 monoclonal antibody (Biolegend, San Diego, CA); mouse anti-VACM1 (MR106, Ebioscience, San Diego, CA); goat anti-rabbit FITC (A-32731), goat anti-mouse FITC (A-21131), goat anti-rabbit Texas Red (A-11037), goat anti-mouse Texas Red (A-32742) (Invitrogen, Carlsbad, CA); NuPAGE Gels (3–8%, 4–12%, 10%) and Bis-Tris Buffer, sodium acetate buffer, SeaBlue Plus2 protein standard, PVDF membrane, iBlot transfer kit, and iBind Cards (Life Technologies, Carlsbad, CA); AP color reagent and AP conjugate substrate kit (Bio-Rad, Hercules, CA); VECTASHIELD mounting medium containing DAPI (Vector, Burlingame, CA); annexin V-FITC, Dynabeads® protein G kit and BS3 (Invitrogen, CA); lactadherin and lactadherin-FITC (Haematologic Technologies, Essex Junction, VT); mannan (Sigma, St. Louis, MO).

SapC prepared under Good Manufacturing Practices (GMP) and HPLC purified is produced using the pET expression system in *E. coli* cells by the Changji Bio-Tech Company (Changzhou, China). The endotoxin level in the SapC preparations was <0.1 EU/mg, achieving a safety level for clinical use. GCCase is Velaglucerase alfa with mannosyl-terminated chains that is provided by Shire. Characterization of SapC-DOPS nanovesicle has been described previously [32]. The nanovesicle size is measured at ~190–200 nm (Fig. S1) in dimension by photon correlation spectroscopy utilizing a N4 plus particle size analyzer and TEM imaging showed uniform SapC-DOPS nanovesicles. Optimization of the SapC-DOPS-GCCase formulation shown in Tables S1, S2 and Fig. S1, binding of GCCase to SapC-DOPS, determined by Microscale Thermophoresis, shown in Tables S3 and Fig. 1, and estimation of the number of SapC and GCCase molecules are described in supplementary Methods.

2.2. SapC-DOPS-GCCase formulation

SapC and DOPS was mixed at molar ratio 1:7 in 250 μ L 0.1 M Citrate Phosphate (CP) buffer (pH 5.6) with 80 μ g/mL (1.33 μ M) GCCase (1 U = 10 μ g of Velaglucerase alfa, GCCase). The formulation mixture was bath sonicated for 15 mins at 4°C and then diluted to 1 mL with CP buffer.

2.3. GCCase activity assay

Two assay buffer systems were used, a Tc/Tx system (1% Na-taurocholate/1% Triton X-100) for measuring GCCase activity in cell free

SRT agent has shown CNS efficacy in preclinical studies and is in a Phase II clinical trial for GD type 3 [15]. Gene therapy using viral vectors has shown promising results, but significant obstacles limit clinical translation [16–18]. Recent studies using adeno-associated viral (AAV) vectors that express GCCase have shown improvement of CNS disease in GD mouse models [18]. However, immunogenicity and long-term safety of AAV need to be established before applying to patients. Additionally, pharmacological chaperones can enhance the mutant GCCase stability/trafficking [19,20], but selecting non-inhibitory GCCase chaperones for in vivo applications is challenging [21].

Saposin C (SapC) is a small lysosomal glycoprotein derived with three other saposins (A, B and D) from a single precursor, prosaposin. These saposins are present in all nucleated cells [3]. SapC functions as a critical optimizer of GCCase activity, protects GCCase from protease degradation, and prevents GCCase inhibition by α -synuclein [22–25]. Mutations in the SapC codons of the human or mouse prosaposin genes, *PSAP* or *Psap*, respectively, lead to SapC deficiency and GD/nGD-like diseases [3, 26, 27]. SapC deficiency caused GD-like diseases have a much lower frequency than *GBA1*-based GD [27, 28]. A novel complex, SapC-DOPS (SapC coupled with the phospholipid, dioleoyl-phosphatidylserine; DOPS), selectively targets and effectively

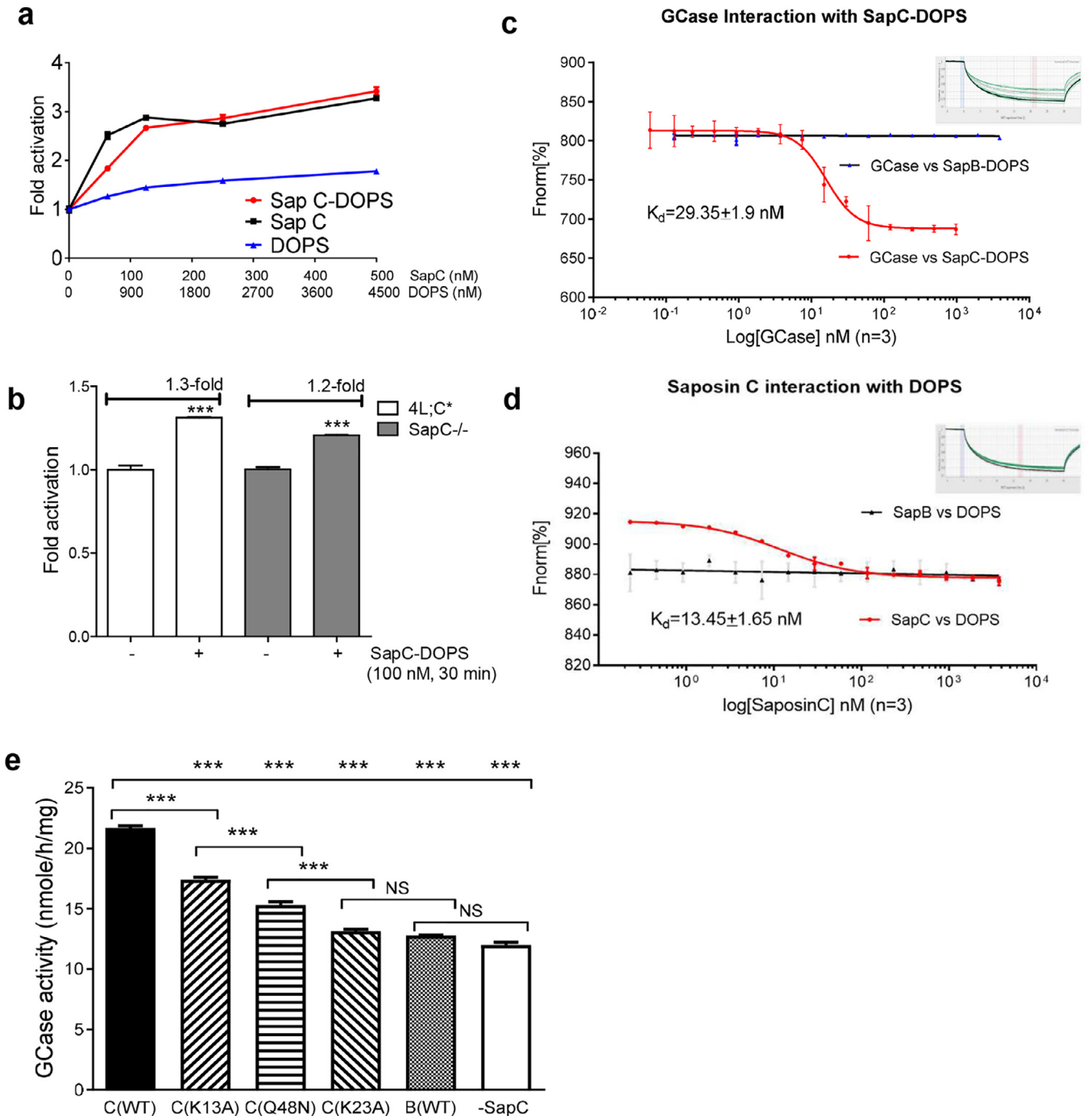


Fig. 1. SapC-DOPS activates GCCase. (a) SapC-DOPS and SapC similarly activate GCCase in a cell-free assay. DOPS is a control. SapC, 0 to 500 nM; DOPS, 0 - 4500 nM. Free GCCase incubated with SapC-DOPS or SapC for 30 min before determining the GCCase activity. (b) SapC-DOPS increases GCCase activity in fibroblasts from SapC-deficient mice (4L;C* and SapC^{-/-}). The cultured cells were incubated with 100 nM SapC-DOPS for 30 min before harvesting for GCCase activity assay. Student's *t*-test. ***, *p* < 0.0001. (c) K_d of GCCase interaction with SapC-DOPS compared to SapB-DOPS. (d) K_d of SapC interaction with DOPS compared to SapB with DOPS. The K_d values were determined by microscale thermophoresis (MST) using Affinity Analysis v2.1.3 software. (e) Functional domain of SapC. GCCase activity in 4L;C* fibroblasts treated with WT SapC, mutant SapCs or WT SapB formulated with DOPS-GCCase. The cells were incubated for 5 days with two changes of fresh medium with the formulation. One-Way ANOVA with Tukey's multiple comparison test. ***, *p* < 0.05. The samples were assayed in triplicates/experiment of 2–3 independent experiments.

assay, serum, cells and visceral tissues (Figs. 1, 2, 3F, S2; Tables S1 and S2). The brain PS (BPS) system (0.5 μM BPS) is used to determine SapC's effect on brain GCCase activity by homogenizing the brains in 1X PBS and incubated in 0.5 μM BPS (Figs. 3D and 5B). The GCCase activity assay was carried out as described [33]. Protein concentrations of cells and tissues were determined by the BCA assay using bovine serum albumin (BSA) as a standard. In the cell-free assays, the dilution of GCCase (Velaglucerase alfa, 1 mg/mL) was 1:2000. The final

concentration of polysorbate 20 was ~ 4 nM which has no impact on GCCase activity [34].

2.4. Cell culture

Fibroblasts from *Gba1* null (*Gba1*^{-/-}), 4L;C* (see below) and SapC deficient (C^{-/-}) mice [35–37] and human GD types 2 and 3 patient fibroblasts (GM1260: *GBA1* L444P/P415R and GM877: *GBA1* L444P/

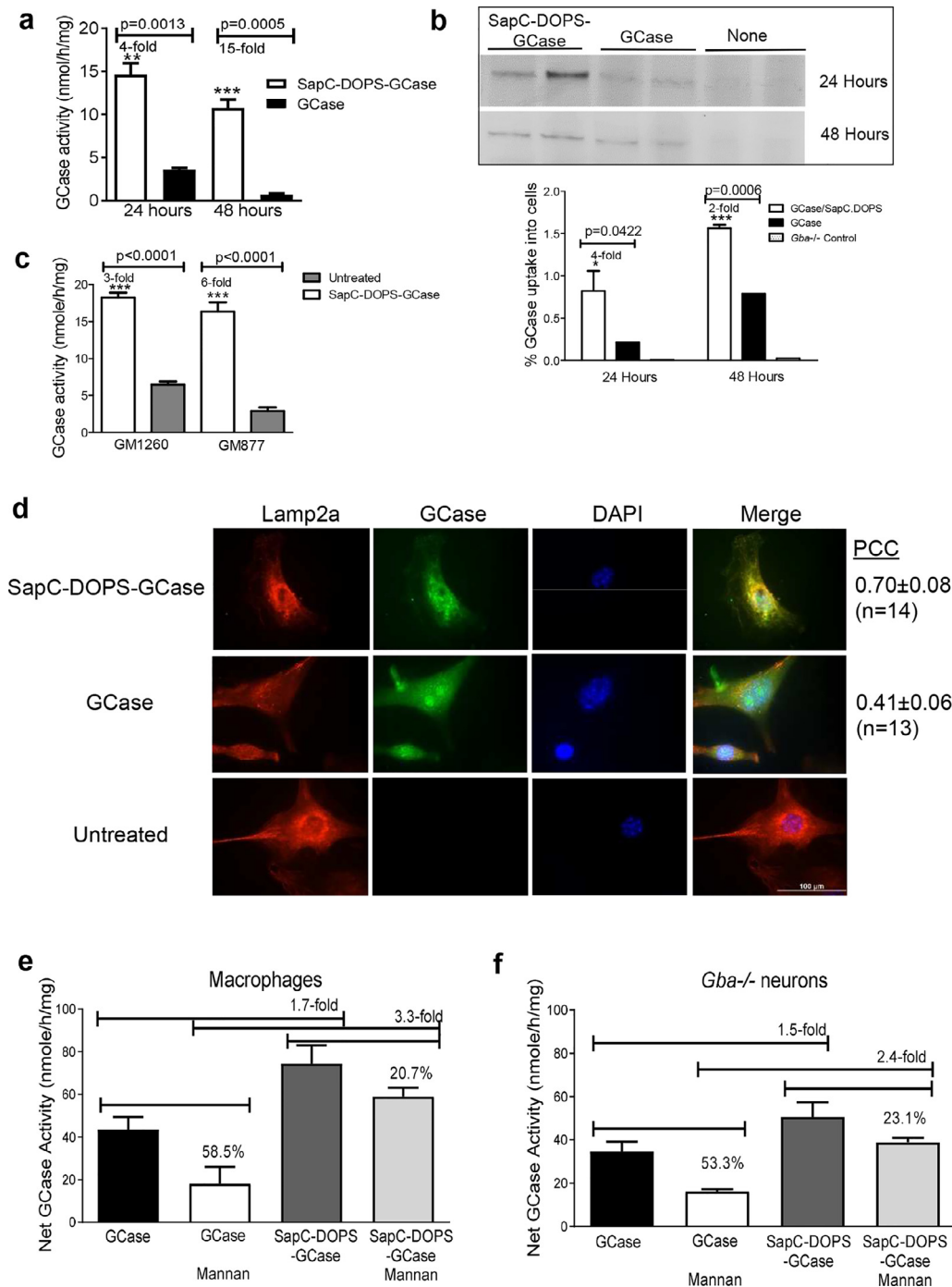


Fig. 2. SapC-DOPS nanovesicles preserve GCCase. Cellular GCCase activity (a) and GCCase protein (b) of mouse *Gba1*^{-/-} fibroblasts that were incubated for 24 or 48 h with SapC-DOPS-GCCase and GCCase, respectively. SapC-DOPS-GCCase incubated cells showed higher levels of GCCase activity and protein than GCCase incubated cells. (c) GCCase activity of human GD2 and GD3 fibroblasts, GM1260 (L444P/P415R) and GM877 (L444P/L444P), incubated with SapC-DOPS-GCCase for 24 h. (d) Human GCCase (green) detected in the lysosome (Lamp2a, red) of *Gba1*^{-/-} fibroblasts incubated with SapC-DOPS-GCCase and GCCase for 24 h. The cells with SapC-DOPS-GCCase showed higher PCC (Person correlation coefficient) compared to GCCase incubated cells ($n = 8 - 14$ cells), indicating more GCCase targeting to lysosomes in SapC-DOPS-GCCase incubated cells compared to free GCCase incubated cells. Scale bar = 100 μm for all images. (e) Effect of mannan on GCCase uptake. J774E macrophages and *Gba1*^{-/-} neurons were incubated with 80 μg GCCase/mL of SapC-DOPS-GCCase or free GCCase in the presence and absence of mannan (2 mg/mL). All the cells used for the assays were washed prior to collection. The data presents net GCCase activity (increased GCCase activity level minus basal/endogenous GCCase activity level). The samples were assayed in triplicates/experiment of 2–3 independent experiments.

L444P, Coriell Institute, Camden, NJ) were cultured in DMEM with 10% FBS. Transformed *Gba1*^{-/-} neurons, kindly provided by Dr. Ellen Sidransky at NIH [38], were maintained in Neurobasal Medium (Gibco, Carlsbad, CA). Macrophage mannose receptor positive, J774E macrophage cell lines were maintained with 10% FCS/DMEM as described [39]. For GCCase uptake experiments, the cells (1×10^6 cells/well) were incubated for 24 or 48 h, or 5 days (with two changes

of fresh medium with the formulation) with equal amounts of GCCase protein (80 μg /mL) as SapC-DOPS-GCCase or as free GCCase freshly prepared in 0.1 M CP buffer (pH5.6). GCCase activity and protein concentration were determined [33]. The cells cultured on chamber slides were processed for lysosomal localization of GCCase by immunofluorescence using Lamp2a as a lysosomal marker. For mannose receptor-mediated GCCase uptake experiments: J774E and *Gba1*^{-/-} neuron

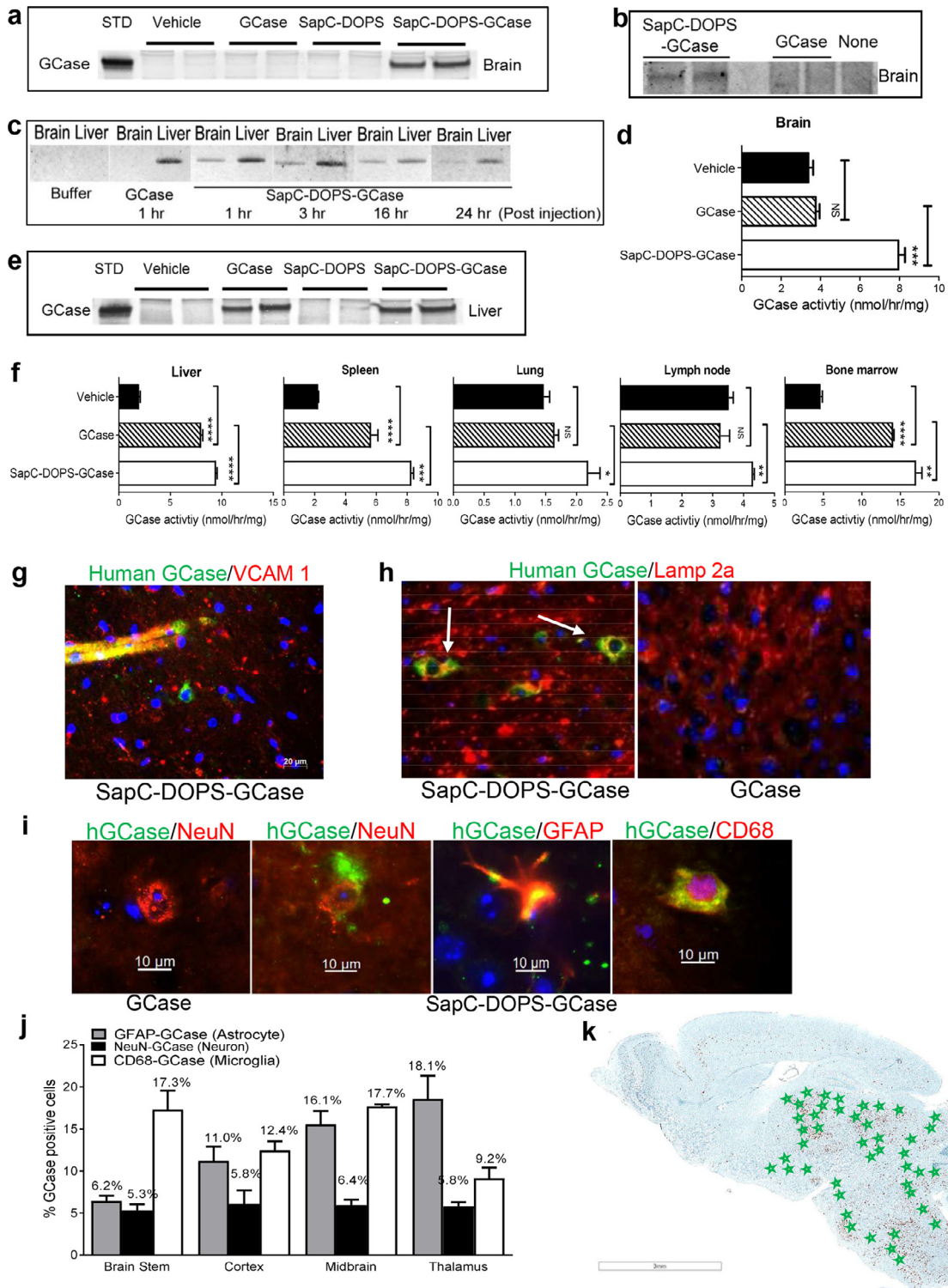


Fig. 3. Tissue distribution of SapC-DOPS-GCCase. (a to e) 4L;C* and WT mice at 38 days of age were i.v. infused with one bolus injection of SapC-DOPS-GCCase, vehicle (CP buffer) or free GCCase (54.6 mg/kg SapC-DOPS and 0.4 mg/kg free GCCase; 0.4 mg/kg free GCCase). Tissues were collected 3 h post injection or as indicated. (a to c) GCCase protein detected by immunoprecipitation followed with immunoblot in 4L;C* (a) and WT (b) brains with SapC-DOPS-GCCase. (c) GCCase protein detected in the 4L;C* brains and livers at 1 to 24 h post injection with SapC-DOPS-GCCase. (d) GCCase activity increased in SapC-DOPS-GCCase treated brains. (e) GCCase protein detected in the 4L;C* liver. Human GCCase (20 ng) is a loading control in A and E. (f) GCCase activity in 4L;C* mouse tissues at 49 days of age treated with SapC-DOPS-GCCase, free GCCase or vehicle-CP buffer (2 h post i.p. injection of, 2 x injection/2 h). SapC-DOPS-GCCase was distributed to liver, spleen, lung, lymph nodes and bone marrow cells. SapC-DOPS-GCCase-treated mice have significantly higher activity in those tissues than free GCCase-treated mice. (g-k) Distribution of human GCCase in brain regions of 4L;C* mice at 38 days of age treated with SapC-DOPS-GCCase or free GCCase (3 h post one bolus i.v. injection). (g) Human GCCase (green) co-stained with VCAM 1 (red) positive endothelium by immunofluorescence (IF) in SapC-DOPS-GCCase treated 4L;C* mouse brain. Scale bar is 20 μm. (h) Human GCCase (green) detected by IF in the lysosome (Lamp2a, red) of brain cells. No GCCase is detected in free GCCase treated 4L;C* brains. Image magnifications are 400x. (i) Panel: representative images of GCCase protein (green) detected by IF in astrocytes (red, GFAP), neurons (red, NeuN) and microglia (red, CD68) in SapC-DOPS-GCCase-treated 4L;C* mouse brains. Scale bar = 10 μm for all images. (j) The graph shows the percentage of brain cells containing GCCase. (k) Human GCCase positive cells (green stars) determined by IF were distributed in 4L;C* mouse brain regions that show inflammation stained with anti-CD68 (brown). Hematoxylin stains nuclei (blue). Scale bar is 3 mm. n = 3 mice, replicated assays of 2-3 independent experiments, n > 5 images/mouse. Student's t-test. *, p < 0.05; **, p < 0.01; ***, p < 0.001.

cells were treated with a mannose receptor inhibitor, mannan (2 mg/ml) overnight. The cells were collected and washed with glycine (0.9%)/saline to remove the surface attached GCCase prior to GCCase activity measurement. All the cells used in the activity assay were washed prior to collection.

2.5. SapC-DOPS-GCCase serum/medium stability

Freshly formulated SapC-DOPS-GCCase in CP buffer (pH 5.6) was tested for its stability in serum (pH 7.4) from wild type (WT) mice and DMEM medium (pH 7.2, 10% FCS) over 8 h. GCCase activities were measured at 0, 1, 2, 4, 6 and 8 h with the Tc/Tx system. The same amount of free GCCase was set as a control to compare its activity versus SapC-DOPS-GCCase at same condition. The assays were repeated twice, each in triplicates. EC50 was calculated using GraphPad Prism 7.

2.6. Immunoprecipitation (IP) of GCCase

IP was performed using Dynabeads® protein G kit to quantify human GCCase protein in the mice. Protein G was prepared by cross-linking the trapping antibody, rabbit anti-human GCCase [40] using bis(sulfosuccinimidyl) substrate (BS3, Thermo-Fisher). Mouse brain or liver lysates (1 mg protein from nGD mice and 10 mg protein from WT mice) were mixed with 80 μ L of protein G beads cross-linked with anti-GCCase antibody and incubated at 4°C overnight. GCCase was eluted from the beads using glycine, pH ~7.2 - 8 and analyzed by immunoblot. Following elution, the beads were denatured with SDS buffer and showed no detectable GCCase.

2.7. Immunoblotting

The cells and tissues were homogenized in Mammalian-Protein Extraction Reagent (M-PER) and subjected to electrophoresis on 4–12% NuPAGE gels. The proteins were transferred to PVDF membranes using an iBlot 2 gel transfer device (Life Technologies). The blots were incubated with rabbit anti-human GCCase antibody (1:1000) [40] or anti- β -actin (1:5000) antibody overnight at 4°C in 1.5% BSA/1.5% milk/PBS buffer. GCCase (Velaglucerase alfa) was used as positive control or a protein quantitation standard (10, 20 and 40 ng protein) and loaded on the same gel with the samples. The IP GCCase was analyzed using goat anti-human GCCase antibody. The signals were detected with AP Conjugate Substrate Kit. Optical densities of protein bands on the immunoblots were quantified by Image J 1.51j4 (NIH, Bethesda, MD).

2.8. GD mouse model and treatment

4L;C* mice harbor V394L/V394L *Gba1* (4L) and *sapC*^{-/-} (C*) homozygosity. The 4L;C* mice were originally generated in the background of C57BL/6J/129SvEV [36]. To minimize mixed background interference with behavioral testing, a C57BL/6J strain of 4L;C* mice was generated. Here, 4L;C* mice in the C57BL/6J background were generated by first crossing of V394L/V394L *Gba1* and *sapC*^{-/-} in C57BL/6J/129SvEV with WT C57BL/6J mice for 10 generations, and then back-crossing of C57BL/6J V394L/V394L *Gba1* and C57BL/6J *sapC*^{-/-}. The C57BL/6J 4L;C* mice developed the same neurological phenotype as C57BL/6J/129SvEV 4L;C* mice and with an average life span of ~56 days. These mice have a sufficient lifespan to allow for the current studies of biochemical correction of GCCase deficiency by SapC-DOPS-GCCase and to assess phenotype improvement by these treatments.

The 4L;C* mice were treated with SapC-DOPS-GCCase, free GCCase or vehicle at 10 μ l/g body weight. Starting day 21, when the tail vein was not accessible, the formulation was administered by daily intraperitoneal (i.p.) injections at dose of total SapC-DOPS (109.2 mg/kg)

with GCCase (0.8 mg/kg). Tail vein of intravenous (i.v.) injection started at day 28, 3 times per week, at a dose of total SapC-DOPS (54.6 mg/kg) and GCCase (0.4 mg/kg). The parallel control mice were either not injected, injected with vehicle (CP buffer or saline), free GCCase in CP buffer (i.p.-0.8 mg/kg, i.v.-0.4 mg/kg) or SapC-DOPS (i.p.-109.2 mg/kg, i.v.- 54.6 mg/kg). In some experiments, the mice were administered with acute i.p. or i.v. dosing as indicated in the figure legend. Mouse body weights were recorded daily. The mice were monitored for survival and assessed for phenotype development during the treatment and used for analysis of GCCase activity, protein and substrate, and brain pathology. The non-4L;C* littermates (4L;WT and 4L;C^{-/-}) do not show abnormal behavior or pathology and have a normal life span [15, 36]. The strain and age-matched WT mice and non-4L;C* littermates were used as controls. We did not observe gender differences in preliminary studies; age and strain matched mice of both genders were included in all the analyses. All mice were housed under pathogen-free conditions in the animal facility according to IACUC approved protocol (2018–0056) at Cincinnati Children's Hospital Research Foundation.

2.9. CellVue maroon (CVM) in K14-VEGFR3-Ig

The K14-VEGFR3-Ig mouse is a brain microlymphatic mouse model. K14-VEGFR3-Ig mice were obtained from Drs. Kari Alitola (University of Helsinki, Finland) and Melody Swartz (Institute for Molecular Engineering, University of Chicago, Chicago, IL) [41, 42]. WT and K14-VEGFR3-Ig mice with engrafted orthotropic brain tumors (100,000 LLC-GFP cells) were treated with 250 μ L SapC-DOPS-CVM [SapC = 0.4 mg/mL, DOPS = 0.082 mg/mL, CVM = 0.04 μ M] via the tail vein at 12 days of age. The brains of SapC-DOPS-CVM administered mice were collected 24 h post i.v. injection. CVM signal was observed by IVIS imaging (λ Ex = 640 nm; λ Em = 700 nm, 0.1 s) as described [32].

2.10. Glycosphingolipid analysis

Glucosylceramide (GluCer) and glucosylsphingosine (GluSph) in cells and tissues were analyzed at the Medical University of South Carolina Lipidomics Shared Resource: Analytical Unit. The concentration of GluCer and GluSph in the tissues was normalized to mg tissue weight, and in the cells, was normalized by mg protein of the cell lysate [43].

2.11. Immunohistochemistry

Brain tissues were collected after transcardial perfusion with saline and fixed in cold 4% paraformaldehyde (PFA) for processing frozen blocks. CD68 and GFAP monoclonal antibody staining was as described [44]. CD68 and GFAP signals were quantified using Fiji for ImageJ [44].

2.12. Fluoro-Jade C (FJC) staining

FJC (AG325, Millipore, MA) is a polyanionic fluorescein derivative which selectively binds to degenerative neurons for evaluation of neurodegeneration [45]. Frozen brain sections were air-dried and dipped in 80% ethanol/1% sodium hydroxide, 70% ethanol, and 0.06% potassium permanganate for 5, 2, and 10 min, respectively. The sections were rinsed with distilled water and then incubated with 0.0004% FJC in 0.1% acetic acid for 20 min. FJC staining was detected under a fluorescent microscope at 480 nm excitation and 525 nm emission. Images were acquired through a 20x objective with a Zeiss Apotome 200 M, and the fluorescence of FJC-positive cell signals was quantified using Fiji for ImageJ [44].

2.13. Immunofluorescence

The mouse tissues and the cells on chamber slides were fixed with 4% PFA, permeabilized with 0.3% Triton X-100 in PBS, and quenched with 0.05 M NH₄Cl. The cells were blocked with 1.5% BSA and 1.5% non-fat milk in PBS at room temperature for 1 hr. Frozen PFA fixed tissue sections were treated with 0.3% Triton X-100 in PBS and blocked with 1.5% BSA and 10% goat serum in PBS. Primary antibodies were applied to the cells or tissue sections and incubated overnight at 4 °C. Dilutions of primary antibodies were as follows: rabbit anti-human GCCase (1:200); rat anti-Lamp2a or rat anti-Lamp1 (1:250); rat anti-mouse LYVE1 monoclonal (1:250); mouse anti-GFAP monoclonal (1:250); mouse anti-NeuN monoclonal (1:500); and mouse anti-CD68 monoclonal (1:250). Following washing with PBS plus 0.05% Tween-20 (10 min, 3 times), the samples were incubated for 1 hr at room temperature with secondary antibodies: goat anti-rabbit-FITC (1:500), goat anti-rat or anti-mouse-Texas Red (1:500). The samples were washed as above and mounted with Anti-fade mounting medium with DAPI. Fluorescence signals were acquired with a Zeiss Apotome 200 M. Signals from the images were quantified by Fiji for ImageJ [44].

2.14. Behavioral testing

Sensorimotor function was assessed in the mice by gait analyses as previously described [46]. Hindlimb clasping was tested by tail suspension. The mouse was lifted away from all surrounding objects by grasping tail at the base. Hindlimb position was monitored for 30 secs and scored. Score 0 is when hindlimbs are consistently splayed outward, away from the abdomen. Score 1 is when one hindlimb is retracted toward the abdomen for >50% of 30 secs. Score 2 is when both hindlimbs are partially retracted toward the abdomen for >50% of 30 secs. Score 3 is when hindlimbs are entirely retracted and touching the abdomen for >50% of 30 secs. The mice were tested with 2 trials at each time point, 10 mins, apart between trials.

2.15. Lactadherin administration and CVM quantitation

4L;C* mice at 42–43 days of age were i.v. injected with 100 μ L lactadherin (20 μ g/mouse, $n = 5$), BSA (20 μ g/mouse, $n = 5$) or PBS (100 μ L, $n = 2$). Thirty min later, each mouse was given SapC-DOPS-CVM (200 μ L/mouse) by i.v. injection. Mice were euthanized 3 h after the SapC-DOPS-CVM injection and perfused with saline followed by 4% PFA. Brains and meninges were collected for *ex-vivo* IVIS imaging and post-fixed in 4% PFA for 24 h followed by 30% sucrose for histological studies. CVM signal was observed by IVIS imaging (λ Ex = 640 nm; λ Em = 700 nm; Exposure = 0.5 s) as described [30]. Age, strain and sex matched 4L;C* mice and Non-4L;C* littermate (4L/WT) control mice were injected i.v. with 100 and 200 μ L bovine lactadherin-FITC (83 μ g/mL in PBS). The brain sections were stained with rat-anti-mouse CD68 monoclonal antibody (MCA1957, Bio-Rad, 1:200), anti-Tuj1 or anti-VCAM1 antibodies with secondary antibody conjugated with Texas Red (1:500), respectively. Images of brain sections were acquired with a Nikon C-plus2 microscope and quantification of fluorescence signals on these images were analyzed by ImageJ.

2.16. Statistical analysis

The data were analyzed by Student's *t*-test or ANOVA test, and Log-Rank (Mantel-Cox) test for survival using GraphPad Prism. Figure bars present as mean \pm SEM.

3. Results

3.1. Preparation of SapC-DOPS-GCCase formulation

Both GCCase and SapC are lysosomal proteins that bind phospholipids in the cell membrane [47], thereby providing a rationale to formulate SapC-DOPS with GCCase. Since SapC can enhance GCCase activity [25, 48], the preservation of this SapC function was first determined in SapC-DOPS nanovesicles. GCCase was incubated with various concentrations of SapC-DOPS or SapC and the activity was measured. As shown in Fig. 1a, activation of GCCase by SapC-DOPS is comparable to that by SapC alone. Using SapC-deficient fibroblasts [mouse SapC^{-/-} and mouse 4L;C* harboring V394L/V394L Gba1 (4L) and sapC^{-/-} (C*) homozygosity] [36, 37], SapC-DOPS enhanced GCCase activity by 1.3 fold in 4L;C* and 1.2 fold in SapC^{-/-} fibroblasts (Fig. 1b). Thus, SapC's activation function on GCCase is preserved in SapC-DOPS nanovesicles both *in vitro* and *ex vivo*.

GCCase is rapidly inactivated by neutral pH, but acidic (lysosomal) pH 5.5 preserves GCCase activity [49]. SapC-DOPS with GCCase was formulated in CP buffer (pH 5.6) by routine extrusion technology (Fig. S1a). To determine the maximal GCCase that can be carried by SapC-DOPS, the stoichiometry of GCCase vs. SapC-DOPS and composition of SapC-DOPS were developed by individually optimizing 1) GCCase and 2) DOPS in the formulation. Each formulation was centrifuged to harvest GCCase bound to SapC-DOPS, recovered in the pellet vs. unbound free GCCase in the supernatant. GCCase activity and protein of each bound and free fraction were determined. When SapC (0.1 mM) and DOPS (0.9 mM) were mixed with various amounts of GCCase (0.7 to 1.3 μ M), the highest GCCase activity and protein levels were found in the bound form when 1.3 μ M GCCase was used (Fig. S1b and Table S1). To optimize the DOPS, we tested ratios of fixed SapC (0.1 mM) vs. various amounts of DOPS (0.5–1.1 mM) with 1.3 μ M GCCase. Free and bound GCCase activities and protein are shown in Fig. S1c and Table S2. These results demonstrate that 0.1 mM SapC: 0.7–0.9 mM DOPS is optimal with 1.3 μ M GCCase in the formulation. This SapC-DOPS-GCCase formulation was used in following cell and mice experiments.

3.2. Characterization of SapC-DOPS-GCCase formulation

A strong GCCase and SapC interaction occurs in the presence of unsaturated, acidic phospholipids [25, 48]. Microscale thermophoresis (MST) was used to determine the interaction/binding of GCCase with SapC-DOPS (Supplementary Methods). MST detects the changes in the hydration shell, charge or size of molecules by measuring changes of the mobility of molecules in microscopic temperature gradients [50]. Using fluorescent NBD-phosphatidylserine (PS) as probe in DOPS, GCCase interacted with SapC-DOPS with a binding constant $K_d = 29.35 \pm 1.91$ nM (Fig. 1c and Table S3). As a positive control, the interaction of SapC with DOPS has a $K_d = 13.45 \pm 1.65$ nM (Fig. 1d and Table S3). There were no detectable interactions between GCCase and DOPS, saposin B (SapB)-DOPS or SapC-DOPC (phosphatidylcholine), or between SapB and DOPS, under the same experimental conditions (Table S3). Thus, GCCase has specific binding affinity for SapC-DOPS.

The number of SapC and GCCase molecules in each DOPS nanovesicle is estimated based on the simple geometry and average size measurements for DOPS liposomes (Supplementary Methods). Each DOPS nanovesicle contains an estimated 3.31×10^5 DOPS molecules. In optimized SapC-DOPS-GCCase formulation, about 75% GCCase bound on SapC-DOPS, thus, there are approximately 3.68×10^4 SapC and 3.95×10^4 GCCase molecules in each DOPS nanovesicle.

SapC contains fusogenic/binding (NH₂-region) and GCCase activation (COOH-region) domains [22, 51]. To determine the formulation with maximal uptake of GCCase, SapC-DOPS, SapB-DOPS, and SapC mutant-DOPS were compared by measuring the changes in GCCase activity in 4L;C* fibroblasts following incubation with these

nanovesicles (Fig. 1e). Data from our previous studies show that mutant SapC (K13A) has intact GCCase activation, but defective PS binding activity, mutant SapC (Q48N) does not activate GCCase, but has PS membrane fusogenic/binding activity and mutant SapC (K23A) has neither GCCase activation nor PS binding activities [22, 51]. SapB, as a negative control, does not have fusogenic/binding or GCCase activation functions. These results and our previous studies [22, 51] indicate that SapC in the DOPS nanovesicle retains its GCCase activation function in addition to its fusogenic lipid binding activity potentially allowing it to target PS-exposed brain cells (see below).

3.3. SapC-DOPS-GCCase formulation preserves GCCase activity and facilitates cell uptake

Serum stability of GCCase in the SapC-DOPS-GCCase formulation was determined by measuring GCCase activity in WT mouse sera or culture medium at 0 to 8 h and compared to free GCCase. The half-life or EC50 values showed that SapC-DOPS-GCCase is 3 times more stable than free GCCase in serum and 1.6 times more in culture medium (Fig. S2).

To determine whether SapC-DOPS improves GCCase functionality, SapC-DOPS-GCCase [SapC/DOPS (1:9) mM with 80 μ g/mL GCCase] was assayed for GCCase activity and tested in mouse fibroblasts derived from *Gba1*^{-/-} newborn mice that have no functional GCCase [35]. SapC-DOPS-GCCase and free GCCase with equal amounts of GCCase protein were added to *Gba1*^{-/-} fibroblasts. The cells with SapC-DOPS-GCCase had 4-fold more GCCase activity at 24 h and 15-fold more at 48 h than the cells incubated with free GCCase (Fig. 2a). Cells incubated with SapC-DOPS-GCCase had higher total cellular GCCase protein levels than those with free GCCase at 24 h and 48 h after loading (Fig. 2b). Increased GCCase activity and protein were detected 4 h after loading. Human GD types 2 and 3 patient fibroblasts [52] that have low levels of residual GCCase activity also showed an increase of GCCase activity when incubated with SapC-DOPS-GCCase (Fig. 2c).

SapC-DOPS-GCCase taken up by the *Gba1*^{-/-} fibroblasts was targeted into lysosomes (Fig. 2d), whereas this was less obvious with free GCCase. The co-localization of GCCase with the lysosomal marker, Lamp1, was determined by Pearson Correlation Coefficient (PCC) in the acquired image using Zeiss image analysis software (Fig. S3). The cells with SapC-DOPS-GCCase showed higher PCC (0.70 \pm 0.08) compared to the cells with free-GCCase (PCC = 0.41 \pm 0.06). These results demonstrate that human GCCase formulated with SapC-DOPS is targeted to, and is functional in GD fibroblasts. SapC-DOPS preserves GCCase activity and likely protects GCCase from denaturation, therefore facilitating cellular uptake and lysosomal localization.

3.4. Effect of mannan on uptake of SapC-DOPS-GCCase

Oligo-mannosyl-terminated oligosaccharides on GCCase (e.g., velaglucerase alfa) promote preferential uptake into myeloid-lineage cells expressing the mannose receptor and neurons [53–55]. To determine if cell uptake of SapC-DOPS-GCCase is dependent on the mannose receptor, uptake was assessed with J774E macrophages that express the macrophage mannose receptor and transformed mouse *Gba1*^{-/-} neurons in the presence or absence of mannan, a competitor for the mannose receptor. Both cell types were incubated with equal GCCase, either as free GCCase or as SapC-DOPS-GCCase. The cells were washed thoroughly before the activity assay and confirmed by immunofluorescence that there was no significant GCCase binding on the cell surface. The cells with SapC-DOPS-GCCase showed more GCCase activity than those with free GCCase (Figs. 2e and 2f). Mannan blocked ~50% of free GCCase uptake, but only ~20% of SapC-DOPS-GCCase in either macrophages or neurons (Figs. 2e and 2f). These data suggest that SapC-DOPS-GCCase enters the cells largely through routes other than the mannose receptor, e.g., direct cell membrane fusion.

3.5. Tissue distribution and CNS targeting of SapC-DOPS-GCCase

As mentioned above, mannose-terminated oligosaccharides promote cellular uptake of GCCase via the mannose receptor. However, several organs are poorly or inaccessible to these agents, including the brain, alveoli of the lungs, and lymph nodes [12, 56]. To assess the ability of SapC-DOPS-GCCase to enter the brain and visceral tissues, 4L;^{C*} mice were intravenously (i.v.) or intraperitoneally (i.p.) infused with equal amounts of protein (equal activity) of free GCCase or SapC-DOPS-GCCase. Their activities were kept constant in each experiment. In acute experiments, tissue GCCase protein and activities were determined at 3 h, or as indicated in Fig. 3, post injection. Brain accessible SapC-DOPS-GCCase was confirmed by immunoblot. Human GCCase protein in the brain lysates was immunoprecipitated using our specific rabbit anti-human GCCase antibody (no cross-reactivity with mouse GCCase) followed by immunoblotting with goat anti-human GCCase (Fig. 3a). In comparison, human GCCase protein was detected in the liver of free GCCase and SapC-DOPS-GCCase injected mice (Fig. 3e). SapC-DOPS-GCCase was also delivered into WT mice brains, but at much lower levels than nGD mice (Fig. 3b). GCCase protein in 4L;^{C*} brains was detected up to the end point (24 h post-injection) of the experiment (Fig. 3c). Mice injected with SapC-DOPS-GCCase showed GCCase activity in the brain, but those injected with free GCCase did not, indicating that SapC-DOPS allowed GCCase access into the brain (Fig. 3d).

In visceral tissues, GCCase activity was determined in SapC-DOPS-GCCase i.p.-injected mice. Higher GCCase activity was detected in the liver, spleen, lung, lymph nodes and bone marrow of SapC-DOPS-GCCase injected mice than free GCCase-injected mice suggesting that SapC-DOPS protects GCCase from rapid clearance by the reticuloendothelial system. It also protects GCCase from pH inactivation in serum as evidenced by the long half-life of 0.68 h in the serum (Fig. S2). Liver lysate showed greater incorporation of SapC-DOPS-GCCase than free GCCase to liver (Figs. 3e and 3f). By contrast, in comparison to free GCCase injected tissues, SapC-DOPS-GCCase-injected mice had increased GCCase activity in lymph nodes and lung (Fig. 3f).

In SapC-DOPS-GCCase-treated 4L;^{C*} brains, GCCase was observed lining the endothelium of blood vessels in the treated 4L;^{C*} brain (Fig. 3g). GCCase was trafficked into the lysosome in the brain cells of the 4L;^{C*} mice that had been administered SapC-DOPS-GCCase, but not free GCCase (Fig. 3h). GCCase signals were in ~6% of neurons, 6–18% of astrocytes and 8–18% microglia cells counted in each brain region (Fig. 3i and j). GCCase target cells were distributed mainly in the cortex, midbrain, brain stem and thalamus (Fig. 3j and k). GCCase was co-localized with SapC in treated mouse brain cells demonstrating that GCCase is delivered by SapC-DOPS nanovesicles into the brain (Fig. S4). These results confirm that SapC-DOPS-GCCase entered the brain cells when infused i.v., a clinically relevant, non-invasive procedure for GD treatment.

3.6. SapC-DOPS-GCCase mitigated neuronal phenotypes in nGD mouse model, 4L;^{C*} mice

The 4L;^{C*} model is viable analog of human nGD that have progressive accumulation of substrates and CNS manifestations [36, 57]. 4L;^{C*} mice has a *Gba1* mutation V394L/V394L and lack of SapC [36]. 4L;^{C*} the mice used in this study are in the C57BL/6J background with a median life span of 56 days. SapC-DOPS-GCCase was administered to 4L;^{C*} mice for evaluation of in vivo efficacy. The SapC-DOPS-GCCase formulation used for mice injection was routinely assayed for GCCase activity and a confirmed ~80% GCCase activity remained prior to use. In preliminary studies, SapC-DOPS-CVM and SapC-DOPS-GCCase were delivered into young (13 day old) 4L;^{C*} brains by i.p. injection. Before day 28, when the tail vein was not accessible, the formulation was administered by daily i.p. injections. Tail vein i.v. injection started at day 28 and 3 times per week. The treatment started when disease signs appeared around 21 days.

Treatment effect was evaluated in 4L;*C** mice by neurological phenotype, inflammation, neurodegeneration, and substrate reduction. 4L;*C** mice developed age-related hindlimb clasp behavior. 4L;*C** littermates that have normal phenotype are used as controls to assess clasp behavior change in 4L;*C** mice with treatment. The treated 4L;*C** mice showed significantly delayed hindlimb clasp (Fig. 4a). 4L;*C** mice developed hindlimb paralyses with abnormal

gait, a sensorimotor function deficit. Compared to 4L;*C** mice who received vehicle, SapC-DOPS-GCase treated 4L;*C** mice had significantly improved stride length by gait analysis at 50 and 55 days of age (Fig. 4b). The SapC-DOPS-GCase treatment significantly prolonged 4L;*C** survival to a median of 64 days vs. 56 days for untreated mice; a 14% extension compared to untreated 4L;*C** or 15% compared to free GCase and Vehicle-4L;*C** mice (Fig. 4c). Because free GCase

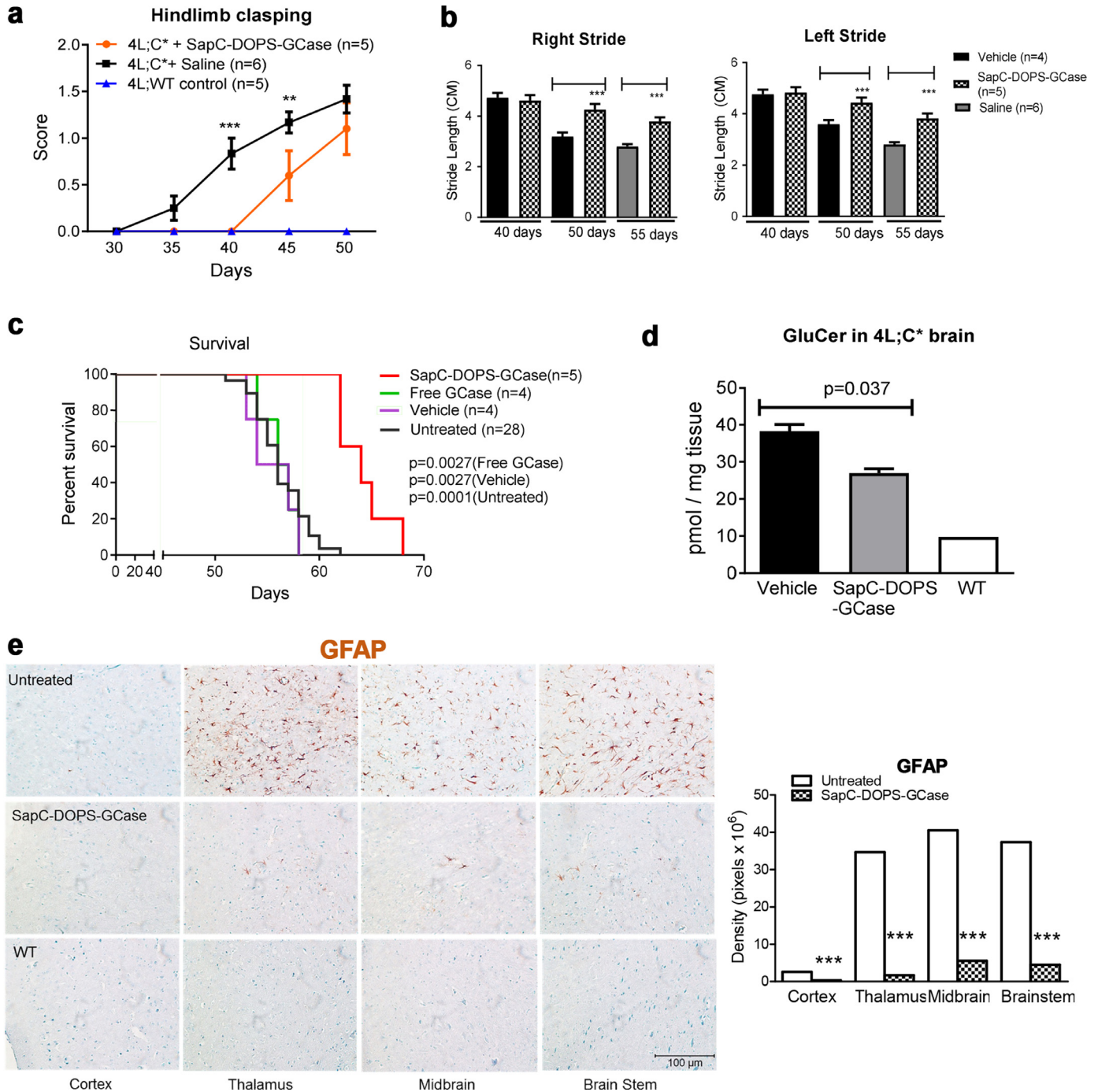


Fig. 4. Therapeutic efficacy of Sap-DOPS-GCase. 4L;*C** mice were treated with SapC-DOPS-GCase and vehicle or free GCase by daily i.p. injections of SapC-DOPS-GCase from day 21 to 27 followed by tail i.v. vein injection from day 28 to terminal age, 3 times per week. (a) Hindlimb clasp was significantly improved in SapC-DOPS-GCase treated 4L;*C** mice compared to saline treated 4L;*C** mice. 4L;WT mice is the normal control. ANOVA test. **, $p < 0.01$; ***, $p < 0.001$. (b) SapC-DOPS-GCase treatment significantly improved right and left strides of 4L;*C** mice at 50 and 55 days of age compared to vehicle (CP buffer) or saline control. Student's *t*-test. ***, $p < 0.001$. (c) Compared to free GCase, vehicle and untreated 4L;*C** mice, SapC-DOPS-GCase treatment significantly prolonged survival of 4L;*C** mice. Log-Rank (Mantel-Cox) test ($p < 0.05$). (d) GCase substrate, GluCer was significantly reduced in treated 4L;*C** brain ($n = 3$, 50 days of age). Student's *t*-test ($p < 0.05$). (e) Treated 4L;*C** brain regions (cortex, thalamus, brain stem and midbrain) showed significantly reduced inflammation determined by anti-GFAP (astrocyte) staining ($n = 3$, 50 days of age). The signal densities of GFAP, were quantified with Image J software and presented as a bar graph. Scale bar is the same for all images. $n > 5$ images /mouse. Student's *t*-test. ***, $p < 0.001$.

does not cross the BBB, as expected, 4L;C* mice administered with free GCCase did not have improved survival and compared to the untreated and vehicle groups (Fig. 4c). The treatment also reduced the substrate, glucosylceramide, accumulation in the brains of 4L;C* mice (Fig. 4d). Brain inflammation was analyzed by anti-CD68 staining on activated microglial cells and anti-GFAP staining on activated astrocytes. SapC-DOPS-GCCase treatment significantly mitigated brain inflammation in 4L;C* mice in the cortex, thalamus, midbrain and brainstem regions (Figs. 4e and S5a). Neurodegeneration, assayed by Fluoro-Jade C (FJC), an anionic fluorescent dye as a marker of degenerating neurons, was significantly diminished in SapC-DOPS-GCCase treated 4L;C* brain stem, midbrain and thalamus regions (Fig. S5b). These data demonstrate improved neuronopathic phenotype in nGD mice by SapC-DOPS-GCCase treatment.

3.7. SapC-DOPS's *in vitro* and *in vivo* efficacy

4L;C* mice have SapC deficiency so the efficacy of SapC-DOPS to replace SapC in 4L;C* mice was evaluated. Increased GCCase activity in SapC-DOPS treated 4L;C* mouse fibroblasts indicates the uptake of SapC is functional (Fig. 1b). Compared to control mice, i.v. injected SapC-DOPS fluorescently labeled with CVM primarily localized to the thalamus of 4L;C* mice (Fig. 5a); this brain region exhibits inflammatory cells in this model [36, 46]. In the control, 4L;WT mice that do not show brain inflammation, low level of CVM was detected (Fig. 5a), suggesting the accessibility of SapC-DOPS into non-inflamed normal brain. To evaluate SapC-DOPS's *in vivo* efficacy, 4L;C* mice were treated with SapC-DOPS, which increased brain GCCase activity (Fig. 5b) and survival (Fig. 5c). Both SapC-DOPS and SapC-DOPS-GCCase improved abnormal gait at 45 days of age in 4L;C* mice (Fig. 5d). While SapC-DOPS alone had small effects on survival of 4L;C* mice, SapC-DOPS-GCCase treated 4L;C* mice showed longer survival and improved gait (Figs. 5c and 5d), signifying enhanced efficacy when GCCase was added to the SapC-DOPS nanovesicles.

3.8. Phosphatidylserine-mediated brain targeting of SapC-DOPS nanovesicles

SapC, a membrane-associated protein, has a favorable binding affinity for unsaturated, negatively charged PS. To determine if SapC-DOPS targeting of 4L;C* brains is dependent on PS, 4L;C* mice were i.v. injected with lactadherin or BSA prior to SapC-DOPS-CVM. Lactadherin is a PS-specific binding protein that acts through its C-2 domain (Lact-C2) [58]. SapC and Lact-C2 both bind PS through its negatively charged head group [47, 59]. Lactadherin cannot enter intact cells so it binds PS only on the outside of the cells [60]. We have previously demonstrated that lactadherin can block SapC-DOPS entry into glioblastoma (brain cancer) cells by shielding the cell surface PS, both *in vitro* and *in vivo* [30]. The CVM signals were detected in the control, BSA injected 4L;C* mice, but were significantly reduced in lactadherin injected mice (Figs. 6a and 6b). Brain cell types that lactadherin binds were determined in the 4L;C* mice i.v. administered with lactadherin-FITC. The lactadherin signals were on active microglial cells (CD68⁺), neurons (Tuj1⁺) and endothelium (VCAM1⁺) (Fig. 6c), but largely absent on astrocytes (GFAP⁺). Lactadherin signals were enriched in a dose-dependent manner in the inflammatory regions that have strong CD68 signals (Fig. 6d). To test whether lactadherin directly inhibits the PS-binding activity of SapC-DOPS nanovesicles, we treated SapC-DOPS-CVM with lactadherin at 37 °C for 30 mins, and collected the pellet after ultracentrifugation to remove free lactadherin. The mixture in the pellet showed the surface PS-binding activity on human brain tumor cells (Gli36) at the same level as the non-lactadherin treated SapC-DOPS-CVM by flow cytometry analysis (Fig. S6). This indicates that free lactadherin cannot significantly reduce the PS-binding effect of SapC-DOPS-CVM. These data support

a PS-mediated pathway via BBB for SapC-DOPS targeting into 4L;C* brain and especially inflamed regions.

3.9. Lymphatic pathway is involved in SapC-based nanovesicles targeting to CNS

To determine the pathway of SapC-DOPS targeting to CNS, SapC-DOPS-CVM was i.v. injected to WT mice. The CVM had a different distribution in brain meninges compared to lectin-stained blood vessels (Fig. S7a), indicating SapC-DOPS does not accumulate in these blood vessels. However, GCCase was detected in mouse brain meninges and co-localized with LYVE1 (lymphatic vessel marker) in 4L;C* mice 24 h after i.v. administration of SapC-DOPS-GCCase (Fig. S7b). CVM infiltrated into lymph nodes in mice i.v. administered SapC-DOPS-CVM (Fig. S7c). Lymphatics-defective transgenic mice, K14-VEGFR3-Ig, develop a lymphedema-like phenotype characterized by edema, swelling of feet and dermal fibrosis but they survive to adulthood despite the lack of lymphatic vessels in several tissues [41, 42]. There is regeneration of the lymphatic vasculature in some tissues but not in the brain where microlymphatics are absent in adult K14-VEGFR3-Ig mice [41, 42]. To test whether the vesicle accumulation in brain is based on the meninges-mediated transport mechanism, we generated orthotopic brain tumors (10 × 10⁵ LLC-GFP cells) in K14-VEGFR3-Ig mice. Long-term SapC-DOPS accumulation was dramatically reduced in brain tumors of these mice (Fig. S7d). Our data indicate that the meningeal-lymphatics are required for SapC-based vesicle uptake in diseased brains and suggest that SapC-based nanovesicles target the CNS through the blood-lymphatic loop [61].

4. Discussion

There is a major unmet medical need for a GD treatment with direct effects on the CNS. Herein, we developed a novel strategy using BBB-penetrating SapC-DOPS nanovesicles through a non-invasive, intravenous administration, to transport functional GCCase into the nGD brain which resulted in therapeutic effects. Formulating GCCase into SapC-DOPS preserved GCCase function and enhanced stability and uptake into cells, primarily via mannose receptor-independent pathways. We also demonstrate that SapC-DOPS-GCCase crosses the BBB of normal and inflamed brains via a mechanism that requires PS-targeting (see diagram in Fig. S8). *In vivo* efficacy of SapC-DOPS-GCCase in a mouse model of nGD showed significant improvement in CNS inflammation, neurodegeneration, survival and neurological phenotype even when the treatment started around onset of disease signs, demonstrating the therapeutic value of SapC-DOPS-GCCase in lessening the nGD.

We have an evidence of binding and activation properties of SapC with GCCase [25]. In this study, GCCase binding to SapC-DOPS revealed a K_d of 29 nM indicating a tight interaction of GCCase with SapC-DOPS nanovesicles. In the SapC-DOPS-GCCase formulation, GCCase is sheltered by the lipid bilayer that allows slow release of GCCase and protects it from rapid denaturation by the neutral pH of plasma or culture media [49] (Figs. 1 and S2), and delays clearance into the reticuloendothelial system (Fig. 3f). EC₅₀ of GCCase in this formulation is three times more than free GCCase in serum (Fig. S2). Thus, SapC-DOPS-GCCase provides a more stable ERT formulation than current ERT agents.

GCCase therapeutics are mannose-terminated recombinantly-produced human enzyme and its cell uptake is preferential for the mannose receptor [53,54]. Reduced mannose receptor-dependency of SapC-DOPS-GCCase suggests that the GCCase has surface and interior membrane occupancy of the SapC-DOPS nanovesicles. Thus, significant amounts of GCCase are delivered through fusion of SapC-based vesicles with the cell and organelle membranes. Consequently, SapC-DOPS-GCCase can access a wider variety of cell types allowing the enzyme into the organs that are inaccessible by ERT, such as lymph nodes, lung and brain (Fig. 3) [12,56]. While ERT has no effect on

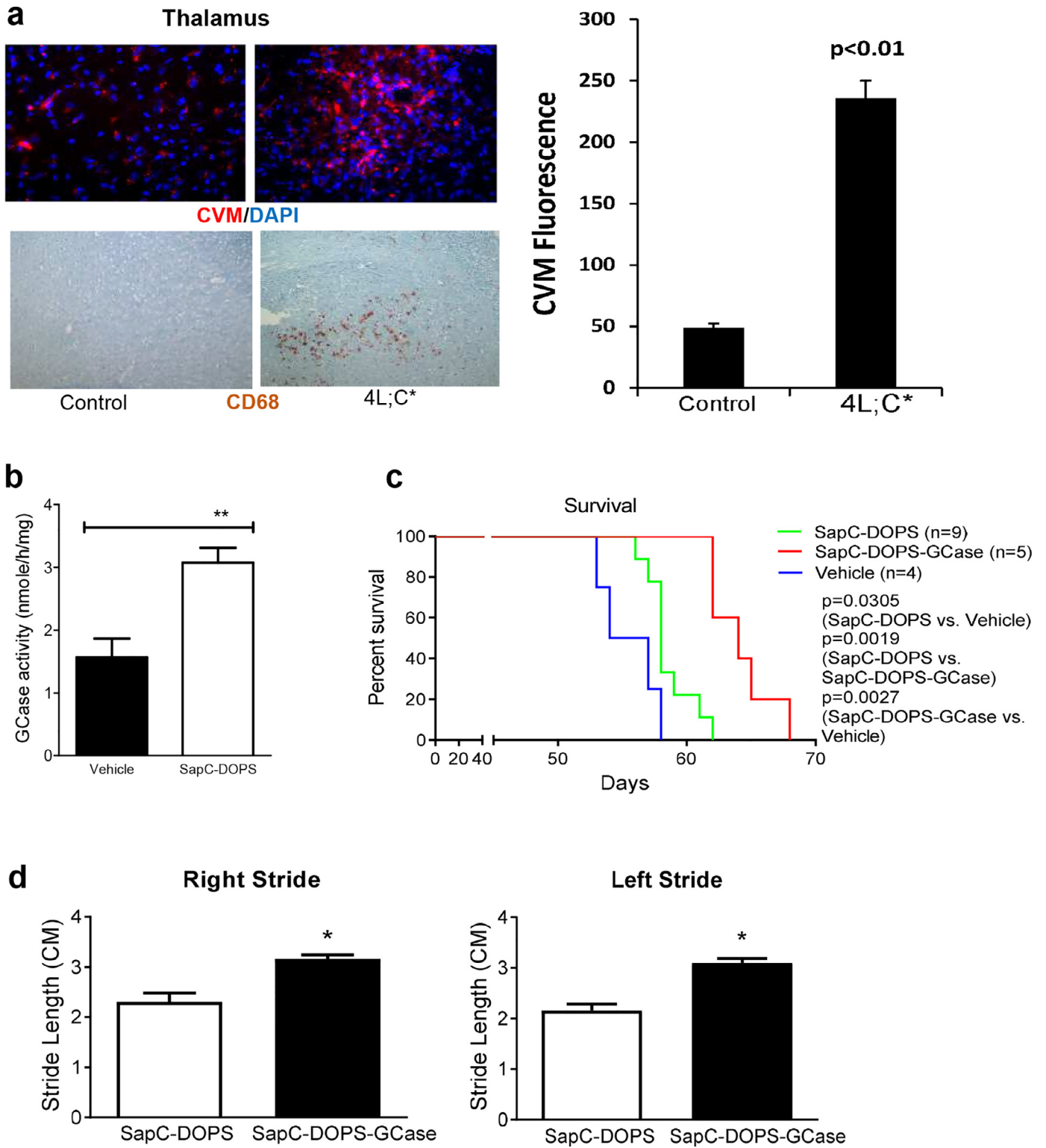


Fig. 5. SapC-DOPS in vitro and in vivo efficacy. (a) SapC-DOPS-CVM (red) detected in the thalamus region of 4L;C* mouse brain that has inflammation stained positive by anti-CD68 (brown). SapC-DOPS-CVM also showed in control 4L;WT mice brain that has no inflammation. Magnification of images are 100x. Bar graph showed CVM levels in 4L;C* and control mice brain in thalamus region. 4L;C* mice at 40 days of age were i.v. injected with 200 μ L SapC-DOPS-CVM (SapC = 0.4 mg/mL, DOPS = 0.082 mg/mL, CVM = 0.04 μ M). Tissues were collected 24 h post injection. (b-d) 4L;C* mice were administered with SapC-DOPS, SapC-DOPS-GCase or vehicle (CP buffer) by daily i.p. injections of SapC-DOPS or SapC-DOPS-GCase from day 21 to 27, followed by tail i.v. vein injection of SapC-DOPS or SapC-DOPS-GCase, 3 times per week, from day 28 to terminal age. (b) Increased GCcase activity in the brain of 4L;C* mice treated with SapC-DOPS (n = 3, 40 days of age). Student's *t*-test. **, *p* < 0.01. (c) SapC-DOPS treated 4L;C* mice showed significantly prolonged survival compared to vehicle-4L;C*. The survival is longer in SapC-DOPS-GCase-treated 4L;C* compared to SapC-DOPS-treated 4L;C* mice. Log-Rank (Mantel-Cox) test (*p* < 0.05). (d) In comparison to SapC-DOPS, SapC-DOPS-GCase treated 4L;C* mice showed significant improved left stride and right stride at 45 days of age (n = 6). Student's *t*-test. *, *p* < 0.05.

lymph nodes in GD type 3 patients [12], SapC-DOPS-GCase accesses lymph nodes (Fig. 3f) and may provide an option for GD patients with massive mesenteric or other lymphadenopathy.

Phosphatidylserine (PS) is normally found on the inner, 'invisible' leaflet of the plasma membrane. SapC, a membrane-associated protein, has a favorable binding affinity with unsaturated, negatively

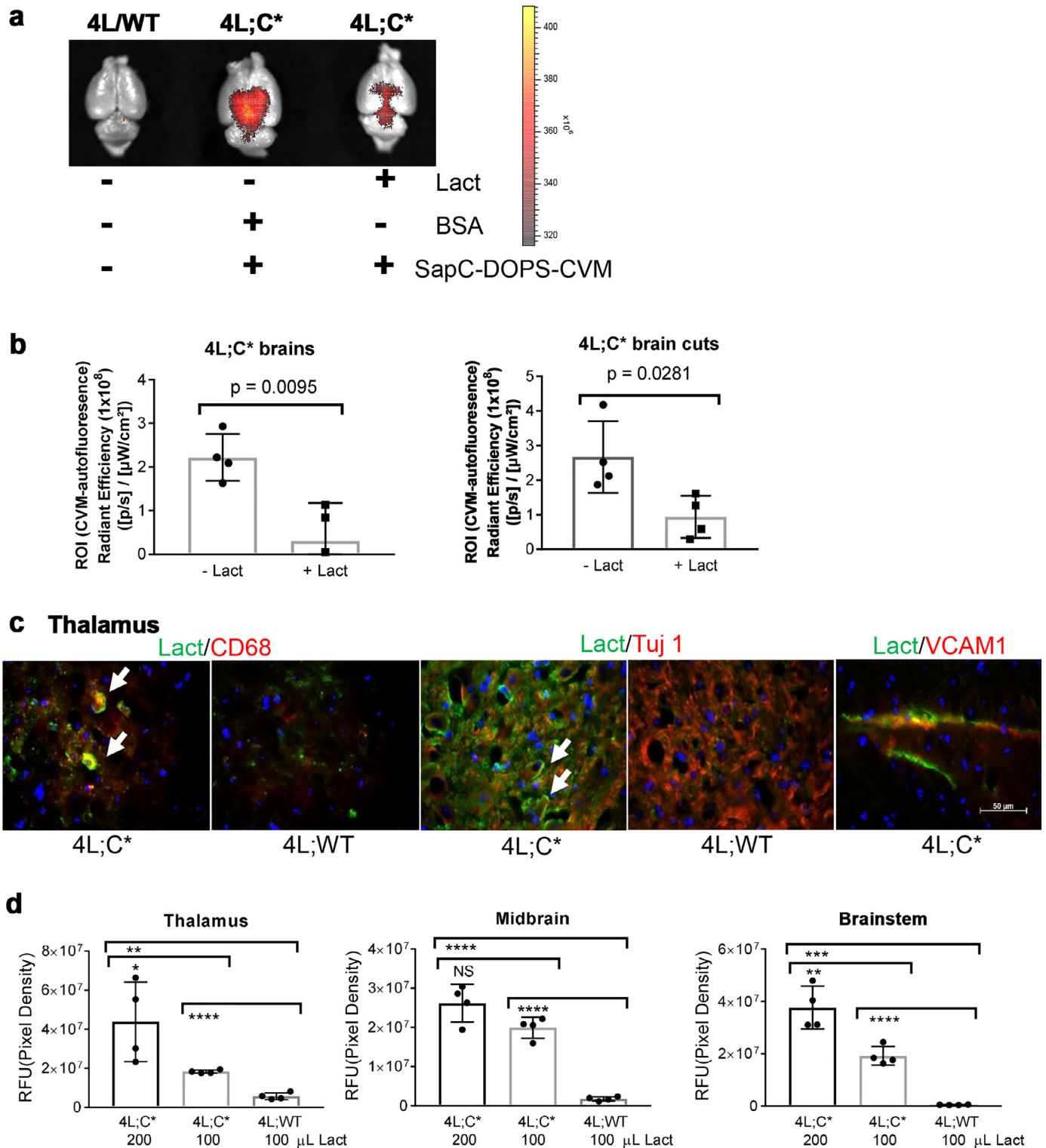


Fig. 6. Phosphatidylserine (PS)-mediated inflamed brain targeting determined by PS-binding protein, lactadherin (Lact). (a and b) Lact blocked SapC-DOPS-CVM targeting into 4L;C* mouse brains. (a) Significantly diminished CVM signals were observed in 4L;C* brains i.v. injected with Lact compared with BSA of whole brain and sagittal brain cuts. Non-symptomatic, non-injected littermate, 4L/WT, brains, used as controls, have no CVM signal. (b) Relative CVM signal levels are shown in the graph. CVM signals were acquired by *ex-vivo* IVIS imaging. Student's *t*-test ($n = 4$ mice). (c and d) Lact distributes in neural cells and inflamed brain regions. 4L;C* and 4L/WT control mice were injected with 100 or 200 μ L of Lact (83 μ g/mL) by i.v. The brain sections were stained with anti-lactadherin-FITC (green) in combination with anti-CD68 (microglia, red), anti-Tuj1 (Neuron, red) and anti-VCAM1 (endothelium, red). (c) Lact signals were around microglia and neuron cells, and on endothelium. (d) Signal levels (RFU, relative fluorescence unit) of Lact in inflamed 4L;C* brain regions. Student's *t*-test ($n = 4$ mice). *, $p < 0.05$; **, $p < 0.01$; ***, $p < 0.001$; ****, $p < 0.0001$.

charged PS. Multiple lines of evidence indicate that inflamed and damaged cells (i.e., apoptotic or necrotic cells) often have abnormal surface PS [62,63]. PS-selective SapC-based nanovesicles are taken up by the brain, especially by PS-exposed enriched inflamed-brains, by

crossing compromised BBB in several neuronal disease mouse models including brain tumor, multiple sclerosis, and epilepsy [30]. As SapC-DOPS targeting is blocked by pre-treatment with the PS-specific binding protein, Lact-C2, such nanovesicles must directly interact

and fuse with the PS-exposed cell membranes and cell surface PS as a major, specific target for SapC-DOPS-GCase (Fig. S7a). PS is a general surface lipid biomarker of inflammatory cells that is suitable for targeted therapy and diagnosis using SapC-based nanovesicles as well as other PS-selective agents.

Nanoscale lipid-based vesicles are taken up by the lymphatic system [64,65]. Indeed, SapC-DOPS nanovesicles or SapC-DOPS-GCase significantly accumulated in mouse spleen, lymph nodes, and liver (Figs. 3 and S7). In prior studies, we have also demonstrated that the nanovesicle was associated with macrophages and neutrophils in inflammatory arthritic joints [29]. Meningeal lymphatics are a reservoir in the CNS blood-lymph circulatory loop [61]. Here, the long-term accumulation of the systemically administered fluorescent SapC-DOPS vesicles in meningeal tissues (Figs. S7a and S7b) was shown and this signal was significantly reduced in the animals with a defective meningeal lymphatic system (Fig. S7d). In addition, the SapC-DOPS-GCase nanovesicles are co-localized with inflammatory cells (microglia/macrophage) from brain (Fig. 4). These findings suggest that SapC-DOPS-GCase may be co-transported by inflammatory cells from the spleen and/or lymph nodes into nGD brains via a compromised blood-lymph circulatory loop (Fig. S8b). This type of loop warrants further investigation.

SapC activates GCase to achieve maximal enzymatic function both in vitro and in vivo [22, 23, 25, 36] and, importantly can induce some GCase mutants to achieve near normal GCase activity [33]. This enhanced activity of mutant GCase stimulated by SapC-DOPS may be therapeutic in selected GD patients who have specific “susceptible” mutations. The GCase activation domain of SapC is localized in the carboxyl-terminal region [22, 66] and the primary physiological function of SapC has been identified from lysosomal storage diseases caused by deficiencies of SapC in humans and mice [28, 37, 67]. Seven cases of a GD-like disease linked to mutations of SapC have been reported in Europe and China [27, 28, 68, 69]. Therefore, therapeutic SapC-DOPS may benefit GD due to defective GCase as well as nGD with SapC deficiency. Our data showed that SapC-DOPS enhances GCase activity *ex vivo* and in vivo (Fig. 5). Notably, SapC-DOPS treatment improved survival and gait abnormalities in 4L;C* mice even when the treatment was started at the age when disease signs appears, demonstrating its CNS efficacy, but SapC-DOPS-GCase showed better effects.

Although ERT is the current standard of care for GD, the available ERT agents do not access particular organs, e.g. brain, lung alveoli, and lymph nodes, and are unable to treat the associated inflammation in such organs [12,70]. Additionally, available ERT agents have no direct effects on nGD since the BBB blocks CNS access to the enzyme. The BBB-penetrating SapC-based nanovesicles developed here delivered exogenous functional GCase into the CNS and establish a potential brain-specific enzymatic therapy for nGD. SapC-DOPS-GCase allows intravenous administration of enzyme treatment for the CNS disease, which has advantages over more invasive procedures, e.g. intracerebral and intrathecal delivery of biologicals into the CNS. SapC-DOPS-GCase provides more benefits than conventional ERT by stabilizing GCase and delivering enzyme into more organs, e.g. brain, lung and lymph nodes that are inaccessible by conventional ERT. Our studies have shown that functional GCase transported by SapC-DOPS nanovesicles is taken up by the inflamed CNS but also by normal brain, which allows SapC-DOPS-GCase treatment at the stages with and without inflammatory breach of BBB. The delivered GCase distributes to the affected regions and reduces substrate accumulation in nGD, subsequently mitigating the phenotype and pathology. While disease improvement was achieved when the treatment started around onset of disease signs, there is a possibility that treatment initiation at a younger age, e.g., postnatal 3 days in this model, could significantly improve the efficacy [15,71]. The basis for the selective CNS regional uptake of SapC-DOPS-GCase in the 4L;C* mice requires additional investigations. The positive outcomes from these

preclinical evaluations in the mouse model of nGD strongly support the translational potential of SapC-DOPS-GCase for GD treatment.

In summary, we developed SapC-DOPS-GCase as a novel therapeutic approach for GD therapy and potentially other lysosomal storage diseases or neurodegenerative disorders. SapC-DOPS-GCase is more stable than conventional ERT and accessible to both visceral and CNS organs, providing a potentially first ERT for managing both CNS and visceral symptoms. This study demonstrates a new mechanism of CNS targeting of SapC-DOPS via a PS-mediated and lymphatic circulation system. SapC-DOPS is a GMP-grade biological and has exhibited a superb safety profile in a Phase 1 clinical trial (ClinicalTrials.gov Identifier: NCT02859857) [72, 73]. The ERT of velaglucerase alfa used in this study is a FDA approved drug for GD treatment. nGD will remain lethal without improvements in treatment but since both of the biological entities have good safety profiles, SapC-DOPS-GCase has the potential to rapidly translate to improved patient care. Although this study was focused on a rare disease, there may be ramifications for similar but more common diseases such as Parkinson disease since decreased GCase activity has been documented in the Parkinson diseased brain, even in patients without *GBA1* mutations [74, 75].

Declaration of Competing Interest

The authors claim a provisional patent application has been filed on March 10, 2020. Consistent with current Cincinnati Children's Hospital Medical Center policies, the development and commercialization of this technology has been licensed to Bexion Pharmaceuticals, LLC, in which X. Qi, holds (< 5%) equity interest.

Acknowledgements

Shire/Takeda provided Velaglucerase alfa for this study. Drs. Kari Alitola and Melody Swartz provided K14-VEGFR3-Ig mice. Dr. Ellen Sidransky provided mouse *Gba*^{-/-} neurons. This study was supported by the National Institutes of Health grants R21NS 095047 to XQ and YS, R01 NS 086134 and UH2 NS092981 in part to YS; Cincinnati Children's Hospital Medical Center Research Innovation/Pilot award to YS and XQ; Gardner Neuroscience Institute/Neurobiology Research Center Pilot award to XQ and YS, Hematology-Oncology Programmatic Support from University of Cincinnati and New Drug State Key Project grant number 009ZX09102-205 to XQ.

Supplementary materials

Supplementary material associated with this article can be found, in the online version, at doi:10.1016/j.ebiom.2020.102735.

References

- [1] Grabowski GA, Petsko GA, Kolodny EH, et al. Gaucher disease. In: Valle D, Beaudet A, Vogelstein B, Kinzler KW, Antonarakis SE, Ballabio A, editors. The online metabolic and molecular bases of inherited diseases. New York: The McGraw-Hill Companies, Inc.; 2010.
- [2] Zimran A, Elstein D, et al. Gaucher disease and related lysosomal storage diseases. In: Kaushansky K, Lichtman M, Prchal J, Levi MM, Press O, Burns L, editors. Williams hematology. 9th ed. New York: McGraw-Hill; 2016.
- [3] Sandhoff K, Kolter T, Van Echten-Deckert G. Sphingolipid metabolism. sphingoid analogs, sphingolipid activator proteins, and the pathology of the cell. *Ann N Y Acad Sci* 1998;845:139–51.
- [4] Gupta N, Oppenheim IM, Kauvar EF, Tayebi N, Sidransky E. Type 2 gaucher disease: phenotypic variation and genotypic heterogeneity. *Blood Cells Mol Dis* 2011;46(1):75–84.
- [5] Conradi NG, Sourander P, Nilsson O, Svennerholm L, Erikson A. Neuropathology of the norrbottnian type of Gaucher disease. Morphological and biochemical studies. *Acta Neuropathol* 1984;65(2):99–109.
- [6] Goker-Alpan O, Giasson BI, Eblan MJ, Nguyen J, Hurtig HI, Lee VM, et al. Glucocerebrosidase mutations are an important risk factor for Lewy body disorders. *Neurology* 2006;67(5):908–10.

- [7] DePaolo J, Goker-Alpan O, Samadpour T, Lopez G, Sidransky E. The association between mutations in the lysosomal protein glucocerebrosidase and parkinsonism. *Movement Disord* 2009;24(11):1571–8 official journal of the Movement Disorder Society.
- [8] Mazzulli JR, Xu YH, Sun Y, Knight AL, McLean PJ, Caldwell GA, et al. Gaucher disease glucocerebrosidase and alpha-synuclein form a bidirectional pathogenic loop in synucleinopathies. *Cell* 2011;146(1):37–52.
- [9] Lachmann RH. Enzyme replacement therapy for lysosomal storage diseases. *Curr Opin Pediatr* 2011;23(6):588–93.
- [10] Platt FM, Jeyakumar M. Substrate reduction therapy. *Acta Paediatr* 2008;97:88–93.
- [11] Bennett LL, Mohan D. Gaucher disease and its treatment options. *Ann Pharmacother* 2013;47(9):1182–93.
- [12] Burrow TA, Sun Y, Prada CE, Bailey L, Zhang W, Brewer A, et al. CNS, lung, and lymph node involvement in Gaucher disease type 3 after 11 years of therapy: clinical, histopathologic, and biochemical findings. *Mol Genet Metab* 2015;114(2):233–41.
- [13] Lukina E, Watman N, Dragosky M, Pastores GM, Arreguin EA, Rosenbaum H, et al. Eliglustat, an investigational oral therapy for Gaucher disease type 1: phase 2 trial results after 4 years of treatment. *Blood Cells Mol Dis* 2014;53(4):274–6.
- [14] Kuter DJ, Mehta A, Hollak CE, Giraldo P, Hughes D, Belmatoug N, et al. Miglustat therapy in type 1 Gaucher disease: clinical and safety outcomes in a multicenter retrospective cohort study. *Blood Cells Mol Dis* 2013;51(2):116–24.
- [15] Marshall J, Sun Y, Bangari DS, Budman E, Park H, Nietupski JB, et al. CNS-accessible inhibitor of glucosylceramide synthase for substrate reduction therapy of neurodegenerative gaucher disease. *Mol Ther* 2016;24(6):1019–29.
- [16] Sands MS, Davidson BL. Gene therapy for lysosomal storage diseases. *Mol Ther* 2006;13(5):839–49.
- [17] Sardi SP, Clarke J, Kinnecom C, Tamsett TJ, Li L, Stanek LM, et al. CNS expression of glucocerebrosidase corrects alpha-synuclein pathology and memory in a mouse model of Gaucher-related synucleinopathy. *Proc Natl Acad Sci U S A* 2011;108(29):12101–6.
- [18] Massaro G, Mattar CNZ, Wong AMS, Sirka E, Buckley SMK, Herbert BR, et al. Fetal gene therapy for neurodegenerative disease of infants. *Nat Med* 2018;24(9):1317–23.
- [19] Lieberman RL, Wustman BA, Huertas P, Powe Jr. AC, Pine CW, Khanna R, et al. Structure of acid beta-glucosidase with pharmacological chaperone provides insight into Gaucher disease. *Nat Chem Biol* 2007;3(2):101–7.
- [20] Maegawa GH, Tropak MB, Buttner JD, Rigat BA, Fuller M, Pandit D, et al. Identification and characterization of ambroxol as an enzyme enhancement agent for Gaucher disease. *J Biol Chem* 2009;284(35):23502–16.
- [21] Aflaki E, Borger DK, Moaven N, Stubblefield BK, Rogers SA, Patnaik S, et al. A new glucocerebrosidase chaperone reduces alpha-Synuclein and glycolipid levels in iPSC-Derived dopaminergic neurons from patients with Gaucher disease and parkinsonism. *J Neurosci* 2016;36(28):7441–52.
- [22] Qi X, Qin W, Sun Y, Kondoh K, Grabowski GA. Functional organization of saposin C. Definition of the neurotrophic and acid beta-glucosidase activation regions. *J Biol Chem* 1996;271(12):6874–80.
- [23] Sun Y, Qi X, Grabowski GA. Saposin c is required for normal resistance of acid beta-glucosidase to proteolytic degradation. *J Biol Chem* 2003;278(34):31918–23.
- [24] Yap TL, Gruschus JM, Velayati A, Sidransky E, Lee JC. Saposin C protects glucocerebrosidase against alpha-synuclein inhibition. *Biochemistry* 2013;52(41):7161–3.
- [25] Qi X, Leonova T, Grabowski GA. Functional human saposins expressed in *Escherichia coli*. Evidence for binding and activation properties of saposins c with acid beta-glucosidase. *J Biol Chem* 1994;269(24):16746–53.
- [26] Pampols T, Pineda M, Giros ML, Ferrer I, Cusi V, Chabas A, et al. Neuronopathic juvenile glucosylceramidosis due to sap-C deficiency: clinical course, neuropathology and brain lipid composition in this Gaucher disease variant. *Acta Neuropathol (Berl)* 1999;97(1):91–7.
- [27] Vaccaro AM, Motta M, Tatti M, Scarpa S, Masuelli L, Bhat M, et al. Saposin c mutations in Gaucher disease patients resulting in lysosomal lipid accumulation, saposin c deficiency, but normal prosaposin processing and sorting. *Hum Mol Genet* 2010;19(15):2987–97.
- [28] Sandhoff K, Kolter T, Harzer K. Sphingolipid activator proteins. In: Scriver CR, Beaudet AL, Sly WS, Valle D, editors. *The metabolic and molecular bases of inherited disease*. iii. 8th ed. New York: McGraw-Hill, Inc.; 2000. p. 3371–88.
- [29] Qi X, Flick MJ, Frederick M, Chu Z, Mason R, DeLay M, et al. Saposin C coupled lipid nanovesicles specifically target arthritic mouse joints for optical imaging of disease severity. *PLoS ONE* 2012;7(3):e33966.
- [30] Blanco VM, Chu Z, Vallabhapurapu SD, Sulaiman MK, Kandler A, Rixe O, et al. Phosphatidylserine-selective targeting and anticancer effects of SAPC-dops nanovesicles on brain tumors. *Oncotarget* 2014;5(16):7105–18.
- [31] Wojton J, Chu Z, Mathysaraja H, Meisen WH, Denton N, Kwon CH, et al. Systemic delivery of SAPC-dops has antiangiogenic and antitumor effects against glioblastoma. *Mol Ther* 2013;21(8):1517–25.
- [32] Qi X, Chu Z, Mahller YY, Stringer KF, Witte DP, Cripe TP. Cancer-selective targeting and cytotoxicity by liposomal-coupled lysosomal saposin C protein. *Clin Cancer Res* 2009;15(18):5840–51 an official journal of the American Association for Cancer Research.
- [33] Liou B, Kazimierczuk A, Zhang M, Scott CR, Hegde RS, Grabowski GA. Analyses of variant acid beta-glucosidases: effects of Gaucher disease mutations. *J Biol Chem* 2006;281(7):4242–53.
- [34] Blonder E, Klibansky C, de Vries A. Effects of detergents and choline-containing phospholipids on human spleen glucocerebrosidase. *Biochim Biophys Acta* 1976;431(1):45–53.
- [35] Tybulewicz VL, Tremblay ML, LaMarca ME, Willemsen R, Stubblefield BK, Winfield S, et al. Animal model of Gaucher's disease from targeted disruption of the mouse glucocerebrosidase gene. *Nature* 1992;357(6377):407–10.
- [36] Sun Y, Liou B, Ran H, Skelton MR, Williams MT, Vorhees CV, et al. Neuronopathic Gaucher disease in the mouse: viable combined selective saposin C deficiency and mutant glucocerebrosidase (V394L) mice with glucosylsphingosine and glucosylceramide accumulation and progressive neurological deficits. *Hum Mol Genet* 2010;19(6):1088–97.
- [37] Sun Y, Ran H, Zamzow M, Kitatani K, Skelton MR, Williams MT, et al. Specific saposin C deficiency: CNS impairment and acid beta-glucosidase effects in the mouse. *Hum Mol Genet* 2010;19(4):634–47.
- [38] Westbroek W, Nguyen M, Siebert M, Lindstrom T, Burnett RA, Aflaki E, et al. A new glucocerebrosidase-deficient neuronal cell model provides a tool to probe pathophysiology and therapeutics for Gaucher disease. *Dis Model Mech* 2016;9(7):769–78.
- [39] Du H, Levine M, Ganesa C, Witte DP, Cole ES, Grabowski GA. The role of mannose-6-phosphate 6-epimerase and the mannose receptor in enzyme replacement therapy. *Am J Hum Genet* 2005;77(6):1061–74.
- [40] Fabbro D, Desnick RJ, Grabowski GA. Gaucher disease: genetic heterogeneity within and among the subtypes detected by immunoblotting. *Am J Hum Genet* 1987;40(1):15–31.
- [41] Mäkinen T, Jussila L, Veikkola T, Karpanen T, Kettunen MI, Pulkkanen KJ, et al. Inhibition of lymphangiogenesis with resulting lymphedema in transgenic mice expressing soluble VEGF receptor-3. *Nat Med* 2001;7(2):199–205.
- [42] Aspelund A, Antila S, Proulx ST, Karlén TV, Karaman S, Detmar M, et al. A dural lymphatic vascular system that drains brain interstitial fluid and macromolecules. *J Exp Med* 2015;212(7):991–9.
- [43] Sun Y, Zhang W, Xu YH, Quinn B, Dasgupta N, Liou B, et al. Substrate compositional variation with tissue/region and GBA1 mutations in mouse models—implications for Gaucher disease. *PLoS ONE* 2013;8(3):e57560.
- [44] Schindelin J, Arganda-Carreras I, Frise E, Kaynig V, Longair M, Pietzsch T, et al. Fiji: an open-source platform for biological-image analysis. *Nat Methods* 2012;9(7):676–82.
- [45] Schmued LC, Stowers CC, Scallet AC, Xu L. Fluoro-Jade C results in ultra high resolution and contrast labeling of degenerating neurons. *Brain Res* 2005;1035(1):24–31.
- [46] Liou B, Peng Y, Li R, Inskip V, Zhang W, Quinn B, et al. Modulating ryanodine receptors with dantrolene attenuates neuronopathic phenotype in Gaucher disease mice. *Hum Mol Genet* 2016;25(23):5126–41.
- [47] Qi X, Grabowski GA. Differential membrane interactions of saposins A and C: implications for the functional specificity. *J Biol Chem* 2001;276(29):27010–7.
- [48] Qi X, Grabowski GA. Acid beta-glucosidase: intrinsic fluorescence and conformational changes induced by phospholipids and saposin C. *Biochemistry* 1998;37(33):11544–54.
- [49] Xu YH, Ponce E, Sun Y, Leonova T, Bove K, Witte D, et al. Turnover and distribution of intravenously administered mannose-terminated human acid beta-glucosidase in murine and human tissues. *Pediatr Res* 1996;39(2):313–22.
- [50] Asmari M, Ratih R, Alhazmi HA, El Deeb S. Thermophoresis for characterizing biomolecular interaction. *Methods* 2018.
- [51] Qi X, Chu Z. Fusogenic domain and lysines in saposin C. *Arch Biochem Biophys* 2004;424(2):210–8.
- [52] Wigderson M, Firon N, Horowitz Z, Wilder S, Frishberg Y, Reiner O, et al. Characterization of mutations in Gaucher patients by cDNA cloning. *Am J Hum Genet* 1989;44(3):365–77.
- [53] Brady RO, Murray GJ, Barton NW. Modifying exogenous glucocerebrosidase for effective replacement therapy in Gaucher disease. *J Inher Metab Dis* 1994;17(4):510–9.
- [54] Van Patten SM, Hughes H, Huff MR, Piepenhagen PA, Waire J, Qiu H, et al. Effect of mannose chain length on targeting of glucocerebrosidase for enzyme replacement therapy of Gaucher disease. *Glycobiology* 2007;17(5):467–78.
- [55] Schueler U, Kaneski C, Murray G, Sandhoff K, Brady RO. Uptake of mannose-terminal glucocerebrosidase in cultured human cholinergic and dopaminergic neuron cell lines. *Neurochem Res* 2002;27(4):325–30.
- [56] Xu YH, Sun Y, Barnes S, Grabowski GA. Comparative therapeutic effects of velaglucerase alfa and imiglucerase in a Gaucher disease mouse model. *PLoS ONE* 2010;5(5):e10750.
- [57] Dasgupta N, Xu YH, Li R, Peng Y, Pandey MK, Tinch SL, et al. Neuronopathic Gaucher disease: dysregulated mRNAs and miRNAs in brain pathogenesis and effects of pharmacologic chaperone treatment in a mouse model. *Hum Mol Genet* 2015;24(24):7031–48.
- [58] Yeung T, Gilbert GE, Shi J, Silvius J, Kapus A, Grinstein S. Membrane phosphatidylserine regulates surface charge and protein localization. *Science* 2008;319(5860):210–3.
- [59] Shao C, Novakovic VA, Head JF, Seaton BA, Gilbert GE. Crystal structure of lactadherin C2 domain at 1.7 Å resolution with mutational and computational analyses of its membrane-binding motif. *J Biol Chem* 2008;283(11):7230–41.
- [60] Shi J, Heegaard CW, Rasmussen JT, Gilbert GE. Lactadherin binds selectively to membranes containing phosphatidyl-L-serine and increased curvature. *Biochim Biophys Acta* 2004;1667(1):82–90.
- [61] Raper D, Louveau A, Kipnis J. How do meningeal lymphatic vessels drain the CNS? *Trends Neurosci* 2016;39(9):581–6.
- [62] Botto M. Phosphatidylserine receptor and apoptosis: consequences of a non-ingested meal. *Arthritis Res Ther* 2004;6(4):147–50.
- [63] Brouckaert G, Kalai M, Krysko DV, Saelens X, Vercammen D, Ndlovu MN, et al. Phagocytosis of necrotic cells by macrophages is phosphatidylserine dependent

- and does not induce inflammatory cytokine production. *Mol Biol Cell* 2004;15(3):1089–100.
- [64] Dixon JB. Lymphatic lipid transport: sewer or subway? *Trends Endocrinol Metab* 2010;21(8):480–7.
- [65] Iqbal J, Hussain MM. Intestinal lipid absorption. *Am J Physiol Endocrinol Metab* 2009;296(6):E1183–94.
- [66] Qi X, Kondoh K, Yin H, Wang M, Ponce E, Sun Y, et al. Ex vivo localization of the mouse saposin C activation region for acid beta-glucosidase. *Mol Genet Metab* 2002;76(3):189–200.
- [67] Christomanou H, Aignesberger A, Linke RP. Immunochemical characterization of two activator proteins stimulating enzymic sphingomyelin degradation in vitro. absence of one of them in a human Gaucher disease variant. *Biol Chem Hoppe Seyler*. 1986;367(9):879–90.
- [68] Christomanou H, Chabas A, Pampols T, Guardiola A. Activator protein deficient Gaucher's disease. A second patient with the newly identified lipid storage disorder. *Klin Wochenschr* 1989;67(19):999–1003.
- [69] Kang L, Zhan X, Ye J, Han L, Qiu W, Gu X, et al. A rare form of Gaucher disease resulting from saposin C deficiency. *Blood Cells Mol Dis* 2017.
- [70] Pandey MK, Burrow TA, Rani R, Martin LJ, Witte D, Setchell KD, et al. Complement drives glucosylceramide accumulation and tissue inflammation in Gaucher disease. *Nature* 2017;543(7643):108–12.
- [71] Sun Y, Ran H, Liou B, Quinn B, Zamzow M, Zhang W, et al. Isofagomine in vivo effects in a neuronopathic Gaucher disease mouse. *PLoS ONE* 2011;6(4):e19037.
- [72] Rixe Olivier, Morris John Charles, Puduvali Vinay K, Villano John L, Wise-Draper Trisha Michel, Muller Carolyn, et al. First-in-human, first-in-class phase 1a study of BXQ-350 for solid tumors and gliomas. *J Clin Oncol* 2018;36(suppl):2517. abstr.
- [73] Cruze Charles A, Rixe Olivier, Morris John Charles, Puduvali Vinay K, Villano John L, Wise-Draper Trisha Michel, et al. Absence of indicators of hypercoagulability and antiphospholipid syndrome in bxq-350 first in human study. *J Clin Oncol* 2018;36(suppl):e14533. abstr.
- [74] Alcalay RN, Levy OA, Waters CC, Fahn S, Ford B, Kuo SH, et al. Glucocerebrosidase activity in Parkinson's disease with and without GBA mutations. *Brain: J Neurol* 2015;138(Pt 9):2648–58.
- [75] Murphy KE, Gysbers AM, Abbott SK, Tayebi N, Kim WS, Sidransky E, et al. Reduced glucocerebrosidase is associated with increased alpha-synuclein in sporadic Parkinson's disease. *Brain: J Neurol* 2014;137(Pt 3):834–48.